Cutting Edge

THE JOURNAL OF IMMUNOLOGY

Cutting Edge: Mechanical Forces Acting on T Cells Immobilized via the TCR Complex Can Trigger TCR Signaling

Ya-Chen Li,*,† Bing-Mae Chen,† Pei-Chun Wu,‡ Tian-Lu Cheng,§ Lung-Sen Kao,¶ Mi-Hua Tao,† Andre Lieber,‖ and Steve R. Roffler†

Engagement of the TCR by antigenic peptides presented by the MHC activates specific T cells to control infections. Recent theoretical considerations have suggested that mechanical forces acting on the TCR may be important for receptor triggering. In this study, we directly tested the hypothesis that physical forces acting on the TCR can initiate signaling in T cells by micromanipulation of individual T cells bound to artificial APCs expressing engineered TCR ligands. We find that mechanical forces acting on T cells bound to APCs via the TCR complex but not other surface receptors can initiate signaling in T cells in an Src kinase-dependent fashion. Our data indicate that T cells are mechanically sensitive when coupled to APCs by the TCR and indicates that the TCR may act as a mechanosensor. Our data provide new insight into TCR function. *The Journal of Immunology*, **2010, 184: 5959–5963.**

The classical TCR is a heterodimer composed of α- and β-chains that are noncovalently associated on the plasma membrane of T cells with CD3, a complex composed of CD3εδ heterodimers, CD3εγ heterodimers, and CD3ζζ disulfide-linked homodimers. The TCR-α/β–chains do not contain signaling domains. Rather, engagement of peptides presented by the MHC (pMHC) by specific TCRs triggers the phosphorylation of tyrosine residues present in the ITAMs of the associated CD3 molecules, which then serve as docking sites for signaling molecules. These proximal events ultimately lead to activation of transcription factors (NF-κB, NFAT, and AP-1) that result in T cell proliferation, differentiation, and cytokine secretion.

Extracellular mechanical forces can facilitate activation of surface receptors and regulate tyrosine phosphatase and kinase signaling (1). An important role for mechanical forces in TCR signaling has also been suggested. For example, actin-driven motility of T cells and shear forces were proposed to promote movement of TCRs into kinase-rich lipid rafts to facilitate TCR signaling (2). Forces that push or twist the TCR/CD3 complex upon ligand engagement have been conceptualized (3, 4). More recently, lateral and vertical forces acting on microclusters of TCR/pMHC complexes on lamellopodium have been suggested to be important for signal transduction (5), and a recent study provides evidence that the TCR can act as an anisotropic force sensor (6). Cytoskeletal forces induced during T cell detachment from APCs have been proposed to initiate TCR signaling (7). Mechanical forces have been suggested to expose CD3ε and CD3ζ cytoplasmic domains for phosphorylation by Lck (8, 9). An important role for force-mediated changes in the TCR has also been proposed based on the structure and interactions of the TCR-α/β–chains and CD3 subunits (10).

Although the idea that mechanical forces can trigger TCRs is an attractive hypothesis, there is a lack of experimental data testing if the TCR is sensitive to mechanical forces. In the current study, a series of artificial APCs expressing defined TCR ligands was employed to directly test if physical forces acting on the TCR could induce T cell signaling.

Materials and Methods

Cells and mice

3T3 murine fibroblasts and Jurkat human T cells were from the American Type Culture Collection (Manassas, VA). Anti-CD28 cells are 3T3 fibroblasts that stably express a membrane-tethered anti-CD28 single-chain Ab (11). Human virus-transformed human fibroblasts (GM00637, Coriell Cell Repositories, Camden, NJ) were generously provided by Dr. T. C. Lee (Institute of Biomedical Sciences, Academia Sinica, Taipei, Taiwan). Spleens were isolated from BALB/c mice maintained under specific-pathogen free conditions in accordance with Institutional Animal Care and Use Committee guidelines.

rDNA

The construction of p2C11-γ1-B7 (CD3L-2d), p2C11-CD44-B7 (CD3L-CD44), and pLNCX-phOx-γ1-B7 (phOx-2d) has been described (12, 13). A DNA fragment coding the ectodomain of CD43 was amplified by RT-PCR of RNA isolated from Jurkat T cells and inserted into the unique SalI site in p2C11-B7 to generate p2C11-CD43-B7 (CD3L-CD43). A his tag was appended to the 3′ end of CD3L-CD43 by PCR to generate soluble CD3L-CD43-his. All transgenes were cloned into pLNCX2 or pLHCX retroviral vectors (BD Biosciences, San Jose, CA).

*Institute of Microbiology and Immunology, National Yang-Ming University; †Institute of Biomedical Sciences, Academia Sinica; ‡Institute of Neurosciences and ¶Faculty of Life Sciences and Institute of Genomic Sciences, National Yang-Ming University, Taipei; §Department of Biomedical Science and Environmental Biology, Kaohsiung Medical University, Kaohsiung, Taiwan; and ‖Division of Medical Genetics, Department of Medicine, University of Washington, Seattle, WA 98195

Received for publication March 12, 2009. Accepted for publication April 8, 2010.

This work was supported by Academia Sinica and Grant NSC96-2628-B001-003-MY3 from the National Science Council, Taiwan.

Address correspondence and reprint requests to Dr. Steve Roffler, Room N232, Institute of Biomedical Sciences, Academia Sinica, Academia Road, Section 2, No. 128, Taipei 11529, Taiwan. E-mail address: sroff@ibms.sinica.edu.tw

The online version of this article contains supplemental material.

Abbreviations used in this paper: AM, acetoxymethyl ester; pMHC, peptide presented by the MHC.

www.jimmunol.org/cgi/doi/10.4049/jimmunol.0900775

Cell transfection

Transient expression of ligands on 3T3 cells employed lipofectamine or calcium phosphate transfection, whereas permanent cells were generated by retroviral infection. After selection in antibiotic-containing culture medium, stable transfectants were sorted on a flow cytometer for similar surface expression of CD3Ls.

T cell binding

T cells prepared from splenocytes as described (14) were labeled 30 min at 37°C with 5 μM calcein-acetoxymethyl ester (AM) (Sigma-Aldrich, St. Louis, MO). A total of 5×10^6 T cells was briefly centrifuged onto CD3L APCs and allowed to bind for 30 min at 37°C. After washing, bound cells were photographed under visible and fluorescence illumination.

Flow cytometry

Purified T cells, 3T3 APCs, and fibroblasts were stained with commercial Abs at the recommended dilutions. The immunofluorescence of 10,000 viable cells was determined on a flow cytometer (PerkinElmer, Waltham, MA).

T cell activation

Defined numbers of mitomycin C-treated CD3L APCs were mixed in triplicate with purified T cells in the presence of 30 ng/ml PMA for 48 h. IL-2 concentrations were measured by ELISA (BD OptEIA kit, BD Biosciences). T cell proliferation was measured by adding 1 μCi [^{3}H]thymidine per well for 16 h before radioactivity was measured in a Topcount scintillation counter.

Calcium mobilization

Calcium mobilization in populations of T cells was measured by mixing 4×10^5 prewarmed APCs and 10^6 T cells prelabeled with 2 μg/ml fluo-4-AM and 5 μg/ml fura Red-AM in PBS containing 0.9 mM $CaCl_2$, 0.5 mM $MgCl_2$, 0.01% Pluronic F-127, 10 μM probenicid, and 1% serum, centrifuging for 40 s at 1400 rpm and then measuring fluorescence on a flow cytometer for 4.5 min at 37°C.

To measure calcium mobilization in individual T cells under shear conditions, T cells were loaded with 1.8 μM fluo-4-AM for 1 h at 37°C. Labeled T cells were allowed to attach for 30 min at 37°C to live CD3L-CD43, CD3L-CD44, or anti-CD28 cells or to glass coverslips coated with rat anti-CD102 (Biolegend, San Diego, CA) or rat anti-CD62L (Serotec, Kidlington, U.K.) Abs. A stream of HBSS was applied to single T cells for 120 s through an ejection micropipette (tip diameter 5 μm) positioned ~10 μm away using a microinjection system (Picospritzer, General Valve, Pine Brook, NJ) under a pressure of 2 pounds per square inch. To examine the specificity of the calcium response in T cells, 10 μM PP2, a potent inhibitor of $p56^{lck}$ and anti-CD3–stimulated tyrosine phosphorylation, was added to fura 2-AM–loaded T cells 30 min before individual T cells were pulsed with fluid.

For T cell pulling experiments, T cells were loaded with 5 μM fura 2-AM (5 mM stock solution in DMSO) in HBSS buffer for 30 min at 37°C in the dark. The T cells were washed twice and then allowed to bind to live CD3L-CD43 or CD3L-CD44 APCs or anti-CD28 cells grown on glass coverslips or to anti-CD62L Ab coated on coverslips. A micropipette (tip diameter 3 μm) was positioned <150 nm (usually within 50 nm) from the surface of individual T cells, and a vacuum (~4 mm Hg) was placed on the pipette for ~10 s to pull the T cell toward the pipette and away from the APC surface.

Calcium responses in individual T cells were measured under a polychromatic xenon lamp light source (Polychrome II, TILL Photonics, Gräfelfing, Germany) coupled to an inverted microscope (IX70, Olympus, Melville, NY). Imaging was performed using a 40× oil immersion objective (Olympus) and a CCD camera controlled by MetaFluor (Molecular Devices, Sunnyvale, CA). T cells were illuminated at 488 nm for fluo-4-AM or at 340 nm and 380 nm for fura 2-AM. Fluorescence emission was captured by time-lapse photography (every second) and analyzed with MetaMorph (Molecular Devices) and Volocity (PerkinElmer) software. Mean values were calculated from three to four independent experiments performed over several months.

Fibronectin immunofluorescence staining

Human and mouse fibroblasts were incubated with rabbit anti-mouse fibronectin polyclonal Ab (AB2033, Millipore, Bedford, MA) and then incubated with FITC-conjugated goat anti-rabbit Ab (ICN Pharmaceuticals, Costa Mesa, CA) before being fixed with 2% paraformaldehyde and stained with 1 μg/ml DAPI in PBS. The coverslips were mounted in 50% glycerol in PBS containing 0.1% antifading reagent and observed under a confocal microscope.

VLA-4 and VLA-5 blocking assay

Mean fluorescence ratios (340/380 nm) of fura 2-AM–loaded T cells bound to CD3L-CD43 APCs in the presence of 20 μg/ml CS-1 peptide (EILDVPST) plus 20 μg/ml GRGDS peptide (Bachem, Torrance, CA) or 10 μg/ml anti–VLA-4 plus 10 μg/ml anti–VLA-5 blocking Abs (Biolegend) with or without micropipette-induced tension on the T cells was measured as described above.

T cell activation of immobilized CD3L-CD43 protein

Soluble CD3L-CD43-his protein (100 μg/ml), purified from stable 3T3 producer cells on Ni Sepharose 6 fast flow (GE Healthcare, Piscataway, NJ), was bound to Ni-nitrilotriacetic acid derivatized glass coverslips. The fluorescence ratio (340/380 nm) of fura 2-AM–loaded B3Z T cells bound to CD3L-CD43 protein with or without micropipette-induced tension on the cells was measured as described above.

Statistical analysis

Significance of differences between mean values was determined by the unpaired *t* test with Welch's correction (Prism, GraphPad, San Diego, CA).

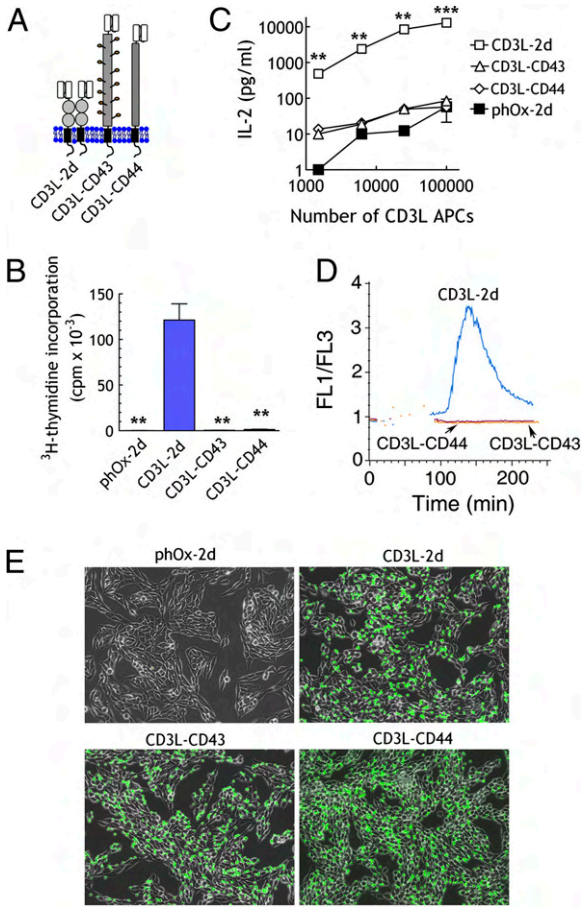

FIGURE 1. Elongated TCR ligands activate T cells poorly. *A*, Illustration of short (CD3L-2d) and elongated (CD3L-CD43 and CD3L-CD44) TCR ligands. *B*, [^{3}H]Thymidine incorporation in 2×10^5 T cells incubated with 2×10^4 CD3L APCs for 48 h ($n = 4$). Bars indicate SEM. phOx-2d is a control nonbinding membrane-anchored scFv similar in structure to CD3L-2d. Significant differences between CD3L-2d APCs and other APCs are indicated. *C*, IL-2 concentrations in culture medium 48 h after 2×10^5 T cells were incubated with graded numbers of CD3L APCs ($n = 3$). Bars indicate SEM. IL-2 secretion induced by CD3L-2d APCs was significantly greater than that induced by other APCs. *D*, Calcium response in fluo-4-AM–labeled T cells incubated with CD3L APCs as measured by the ratio of FL1/FL3 fluorescence. *E*, Monolayers of 3T3 APCs expressing control phOx-2d or the indicated membrane-tethered CD3Ls were incubated with calcein-AM–labeled T cells for 30 min, extensively washed, and then photographed with the fluorescent field overlaying the visible field. Original magnification ×20. $^{**}p < 0.005$; $^{***}p < 0.0005$.

Results and Discussion

We created artificial APCs by tethering a single-chain Ab (scFv) against CD3 (CD3 ligand, CD3L) on the surface of 3T3 fibroblasts, which have a low background of adhesion and costimulatory molecules (Supplemental Fig. 1). CD3L tethered to 3T3 APCs (Fig. 1*A*) via a spacer encompassing two Ig domains linked as preformed dimers via an Ig hinge region (CD3L-2d) induced robust T cell proliferation (Fig. 1*B*), IL-2 secretion (Fig. 1*C*), and intracellular calcium mobilization (Fig. 1*D*). By contrast, elongation of the tether to position CD3L further from the surface of 3T3 APCs by insertion of the extracellular domains of the human CD44 or CD43 molecules (CD3L-CD44 and CD3L-CD43) resulted in poor activation of T cells (Fig. 1*B–D*), consistent with previous reports (14, 15). 3T3 APCs that expressed a negative-control membrane-tethered scFv (phOx-2d) with specificity against a chemical hapten (4-ethoxymethylene-2-phenyl-2-oxazolin-5-one) did not activate T cells, demonstrating the specificity of CD3Ls for T cell activation. Both short (CD3L-2d) and elongated (CD3L-CD43 and CD3L-CD44) ligands effectively bound T cells (Fig. 1*E*), demonstrating that lack of activation by elongated ligands was not due to defects in TCR binding. All of the TCR ligands were also able to form mature immune synapses between APCs and T cells (data not shown). APCs expressing elongated CD3Ls offer an excellent model system to test if physical forces acting on the TCR complex can trigger signaling in T cells because they bind to the TCR complex but do not induce signaling.

To test the hypothesis that TCRs can be triggered by mechanical forces, fluo-4-AM–labeled T cells were first allowed to bind to APCs expressing an elongated CD3L (CD3L-CD43), which does not activate bound T cells under static conditions. A mild perpendicular shear stress was then placed on individual T cells to generate mechanical forces on engaged TCRs, and calcium response, an early hallmark of T cell activation, was monitored (Fig. 2*A*). As expected, fluo-4-AM–labeled T cells bound to CD3L-CD43 APCs under static conditions exhibited only background levels of intracellular fluorescence (Fig. 2*B*, *top row*). By contrast, fluorescence intensity, representing intracellular calcium mobilization, greatly increased in T cells bound to CD3L-CD43 APCs after a mild shear force was placed on the T cells (Fig. 2*B*, *rows 2–4*). As a control, we expressed a membrane-tethered single-chain Ab against CD28 on 3T3 cells (anti-CD28 cells). These cells can bind to CD28 on the surface of T cells. Although T cells bound to anti-CD28 cells, placing the T cells under an equivalent shear force did not induce calcium mobilization in the T cells (Fig. 2*B*, *row 5*), substantiating the requirement for mechanical force to act through the TCR complex. Likewise, T cells prebound to immobilized anti–ICAM-2 or anti-CD62L Abs on glass slides did not exhibit strong fluorescence signals under an identical shear force (Fig. 2*B*, *rows 6 and 7*). Background increases in the fluorescence of negative control cells are likely due to spontaneous dye emission. The mean fluorescence of multiple individual T cells bound to CD3L-CD43 APCs under shear was significantly elevated as compared with bound but static T cells or T cells bound to non-TCR ligands under shear force conditions (Fig. 2*C*). Furthermore, inhibition of Src kinase activity significantly

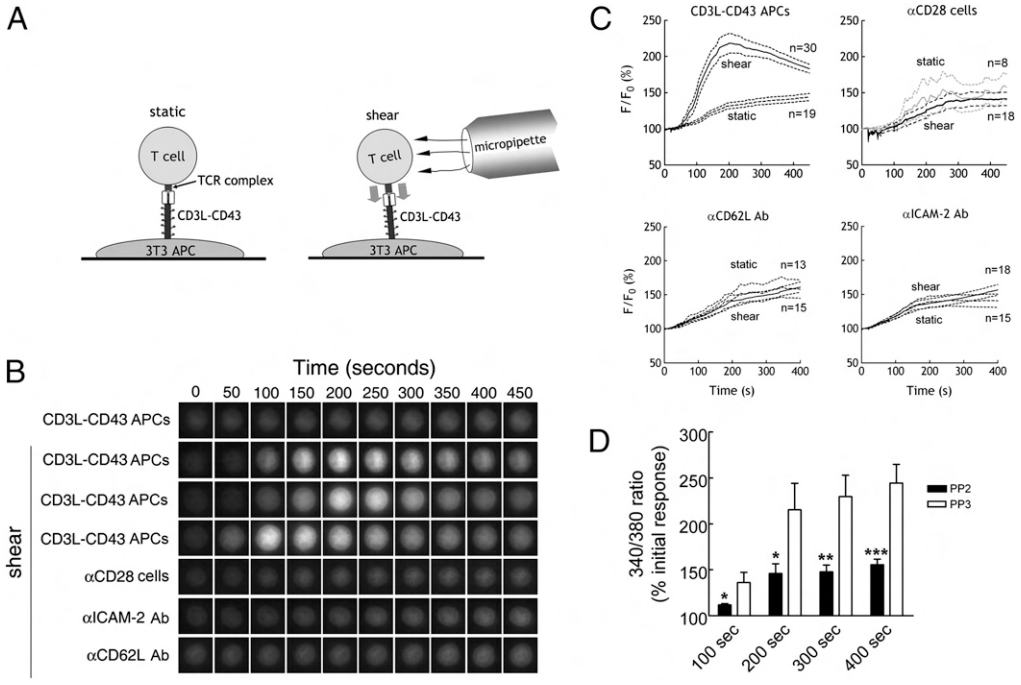

FIGURE 2. Shear forces acting on T cells specifically bound via the TCR complex can induce a calcium response. *A*, Individual T cells bound via the TCR complex to CD3L-CD43 on APCs were pulsed for 120 s with buffer provided via a micropipette placed ~10 μm from the T cell to generate mechanical forces on the TCR complex. *B*, Calcium mobilization in fluo-4-AM–labeled T cells bound to APCs or Ab-coated slides under static (*top row*) or shear conditions (*rows 2–6*) was observed as changes in fluorescence intensity in individual T cells. *C*, Results show the mean fluorescence response of *n* T cells relative to initial fluorescence under shear or static conditions. Only responding T cells in the CD3L-CD43 group are shown (83% of total T cells tested). Dashed lines indicate SEM. *D*, Mean fluorescence response of fura-2-AM–loaded T cells bound to CD3L-CD43 APCs under shear force in the presence of 10 μM PP2 (Src family tyrosine kinase inhibitor) or 10 μM PP3 (negative control inhibitor). Bars indicate SEM. Significant differences between PP2 ($n = 14$) and PP3 ($n = 14$) treated T cells are indicated: $^{*}p < 0.05$; $^{**}p < 0.005$; $^{***}p < 0.0005$.

attenuated calcium mobilization in T cells bound to CD3L-CD43 APCs under shear force conditions (Fig. 2*D*).

We further investigated a role for mechanical force in TCR activation by employing a micropipette to physically pull fura 2-AM–loaded T cells away from APCs (Fig. 3*A*). T cells bound to APCs expressing the elongated TCR ligands CD3L-CD44 or CD3L-CD43 displayed clear calcium responses after the T cells were pulled away from the APCs (Fig. 3*B*). By contrast, tensive forces acting through CD28 or CD62L on the T cells did not increase intracellular calcium levels (Fig. 3*B*). Mean fluorescence values from multiple individual T cells significantly increased when mechanical forces were placed on T cells bound via the TCR complex but not bound to non-TCR receptors (i.e., CD28 and CD62L) (Fig. 3*C*). We ruled out a role for calcium signaling via VLA-4 or VLA-5 interactions with fibronectin deposited on the surface of the APCs (Supplemental Fig. 2). Furthermore, B3Z T cells bound to CD3L-CD43 protein immobilized on glass slides also produced calcium responses to mechanical pulling forces (Supplemental Fig. 3). Taken together, our data demonstrate that physical forces acting on T cells immobilized via the TCR complex, but not the control T cell surface receptors, can initiate signaling in T cells.

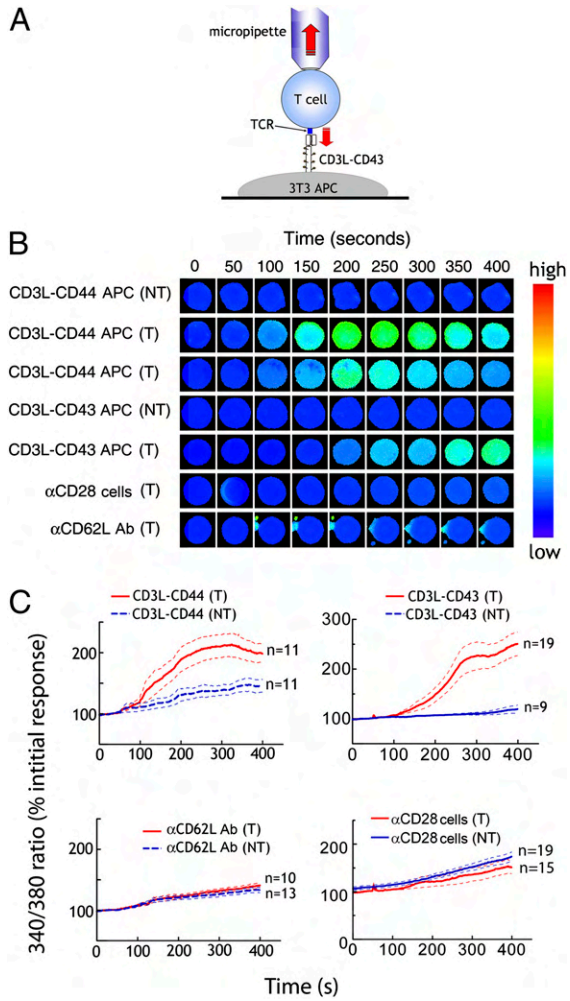

FIGURE 3. Tensive forces on the TCR complex can initiate T cell signaling. *A*, A mild vacuum was applied for ~10 s to an HBSS-filled micropipette positioned near individual fura-2-AM–labeled T cells bound to CD3L-CD43 APCs. *B*, Calcium response of fura-2-AM–loaded T cells bound to APCs or to anti-CD62L Ab-coated glass without (NT) or with (T) micropipette-induced tension on the TCR (CD3L-CD44 or CD3L-CD43 APCs), CD28 (αCD28 cells), or CD62L (αCD62L Ab). *C*, Mean fluorescence ratios (340/380 nm) of all T cells bound to CD3L-CD43 or CD3L-CD44 APCs, anti-CD28 cells or anti-CD62L Ab coated on a glass slide without (NT) or with (T) tension. Eight-five percent of T cells bound to CD3L-CD43 APCs and 93% of T cells bound to CD3L-CD44 APCs produced calcium responses. Dashed lines indicate SEM.

Although we provided external mechanical force, there are several possible physiological sources of mechanical force that may be important for triggering TCR signaling. The TCR and pMHC possess relatively small extracellular domains that project ~7.5 nm from the cell surface, implying that the T cell and APC membranes must approach each other to within ~15 nm at sites of TCR-pMHC engagement (16). The presence of larger molecules near engaged TCRs may act as molecular springs to provide tensive forces on engaged TCRs. Oscillatory movement of the cytoskeleton, forces induced during T cell detachment and migration, or lateral and vertical forces acting on microclusters of TCR-pMHC complexes could also generate forces on the TCR (7, 17). Thermally induced fluctuations in membrane shape that allow comparatively short TCRs to sample pMHC in the presence of large ICAM-1 and LFA-1 molecules (18) or changes in the relative angle between the TCR and CD3 subunits might also generate and transmit forces across the cell membrane (19).

Our study provides direct experimental evidence that the TCR can respond to mechanical forces, offering new insight into TCR function. Combination of biophysical, molecular, and biological studies should help define the relative contributions of various sources of mechanical force and the physiological role of physical force in TCR signaling.

Acknowledgments

We thank John Kung, Konan Peck, Ru-Chi Shieh, and Danny Wang for critical discussions and Qingzong Tseng and Wei-Chen Lu for providing technical assistance.

Disclosures

The authors have no financial conflicts of interest.

References

1. Giannone, G., and M. P. Sheetz. 2006. Substrate rigidity and force define form through tyrosine phosphatase and kinase pathways. *Trends Cell Biol.* 16: 213–223.
2. Lanzavecchia, A., G. Lezzi, and A. Viola. 1999. From TCR engagement to T cell activation: a kinetic view of T cell behavior. *Cell* 96: 1–4.
3. Sun, Z. J., K. S. Kim, G. Wagner, and E. L. Reinherz. 2001. Mechanisms contributing to T cell receptor signaling and assembly revealed by the solution structure of an ectodomain fragment of the CD3 ε γ heterodimer. *Cell* 105: 913–923.
4. Gil, D., W. W. Schamel, M. Montoya, F. Sánchez-Madrid, and B. Alarcón. 2002. Recruitment of Nck by CD3 epsilon reveals a ligand-induced conformational change essential for T cell receptor signaling and synapse formation. *Cell* 109: 901–912.
5. Dustin, M. L. 2007. Cell adhesion molecules and actin cytoskeleton at immune synapses and kinapses. *Curr. Opin. Cell Biol.* 19: 529–533.
6. Kim, S., K. Takeuchi, Z. Sun, M. Touma, C. Castro, A. Fahmy, M. Lang, G. Wagner, and E. Reinherz. 2009. The alphabeta T cell receptor is an anisotropic mechanosensor. *J. Biolog. Chem.* 284: 31028–31037.
7. Ma, Z., P. A. Janmey, and T. H. Finkel. 2008. The receptor deformation model of TCR triggering. *FASEB J.* 22: 1002–1008.
8. Xu, C., E. Gagnon, M. E. Call, J. R. Schnell, C. D. Schwieters, C. V. Carman, J. J. Chou, and K. W. Wucherpfennig. 2008. Regulation of T cell receptor activation by dynamic membrane binding of the CD3epsilon cytoplasmic tyrosine-based motif. *Cell* 135: 702–713.
9. Kuhns, M. S., and M. M. Davis. 2008. The safety on the TCR trigger. *Cell* 135: 594–596.
10. Kuhns, M. S., M. M. Davis, and K. C. Garcia. 2006. Deconstructing the form and function of the TCR/CD3 complex. *Immunity* 24: 133–139.

11. Lee, C. H., Y. H. Chiang, S. E. Chang, C. L. Chong, B. M. Cheng, and S. R. Roffler. 2009. Tumor-localized ligation of CD3 and CD28 with systemic regulatory T-cell depletion induces potent innate and adaptive antitumor responses. *Clin. Cancer Res.* 15: 2756–2766.
12. Liao, K.-W., Y.-C. Lo, and S. R. Roffler. 2000. Activation of lymphocytes by anti-CD3 single-chain antibody dimers expressed on the plasma membrane of tumor cells. *Gene Ther.* 7: 339–347.
13. Cheng, T. L., K. W. Liao, S. C. Tzou, C. M. Cheng, B. M. Chen, and S. R. Roffler. 2004. Hapten-directed targeting to single-chain antibody receptors. *Cancer Gene Ther.* 11: 380–388.
14. Liao, K. W., B. M. Chen, T. B. Liu, S. C. Tzou, Y. M. Lin, K. F. Lin, C. I. Su, and S. R. Roffler. 2003. Stable expression of chimeric anti-CD3 receptors on mammalian cells for stimulation of antitumor immunity. *Cancer Gene Ther.* 10: 779–790.
15. Choudhuri, K., D. Wiseman, M. H. Brown, K. Gould, and P. A. van der Merwe. 2005. T-cell receptor triggering is critically dependent on the dimensions of its peptide-MHC ligand. *Nature* 436: 578–582.
16. Shaw, A. S., and M. L. Dustin. 1997. Making the T cell receptor go the distance: a topological view of T cell activation. *Immunity* 6: 361–369.
17. Alon, R., and M. L. Dustin. 2007. Force as a facilitator of integrin conformational changes during leukocyte arrest on blood vessels and antigen-presenting cells. *Immunity* 26: 17–27.
18. Lee, S.-J. E., Y. Hori, and A. K. Chakraborty. 2003. Low T cell receptor expression and thermal fluctuations contribute to formation of dynamic multifocal synapses in thymocytes. *Proc. Natl. Acad. Sci. USA* 100: 4383–4388.
19. Kuhns, M. S., and M. M. Davis. 2007. Disruption of extracellular interactions impairs T cell receptor-CD3 complex stability and signaling. *Immunity* 26: 357–369.

Legend to Supplementary Figures

Figure S1. Characterization of membrane proteins on 3T3 cells. Live 3T3 cells were stained with the indicated antibodies and appropriate FITC or PE-labeled second antibodies before the immunofluorescence of 10,000 live cells was measured on a flow cytometer (solid lines). Rat anti-mouse CD49d (9C10), rat anti-mouse CD49e (5H10-27) and rat anti-mouse CD102 (3C4) were from BioLegend (San Diego, CA) Rat anti-mouse CD62L (MEL-14) and rat anti-mouse CD44-PE (IM7) were from Serotec (Kidlington, UK). Rat anti-mouse CD2 (RM2-5), hamster anti-mouse CD3ε (145-2C11), rat anti-mouse CD11a (M17/4), hamster anti-mouse CD11c-FITC, rat anti-mouse CD18 (GAME-46), rat anti-mouse CD40-FITC (3/23), rat anti-mouse CD43-FITC (S7), rat anti-mouse CD45-FITC (30-F11), hamster anti-mouse CD48 (HM48-1), hamster anti-mouse CD80-biotin (16-10A1), rat anti-mouse CD86-biotin (GL1), rat anti-mouse I-A/I-E-FITC (2G9), anti-H-$2K^b$ (B8-24-3), mouse anti-fibronectin (clone 10) and mouse anti-hamster IgG-FITC were from BD Biosciences Pharmingen (San Diego, CA). Rat anti-mouse CD54 (BE29G1) was from Biodesign International (Saco, ME). Control antibodies included rat anti-mouse β-glucuronidase (homemade) and mouse anti-rat CD8 α-chain. Goat $F(ab')_2$ anti-rat IgG-FITC and hamster IgG were from Jackson ImmunoResearch (West Grove, PA). Avidin-FITC, goat anti-rabbit-FITC and goat anti-mouse Ig-FITC were from Cappel,

MP Biomedicals (Solon, OH). The immunofluorescence of species-matched negative control antibodies is shown by the shaded curves.

Figure S2. Blocking VLA-4 and VLA-5 does not prevent calcium signaling by tensive forces acting on T cells immobilized via the TCR. A, Human and mouse fibroblasts (10^5/well) were seeded in 24-well plates containing 10 mm coverslips for 24 hours. The cells were washed three times with PBS and blocked with 1% BSA in PBS for 30 min on ice. The cells were incubated 45 minutes on ice with rabbit anti-mouse fibronectin polyclonal antibody (Millipore, AB2033), diluted 20 fold in blocking buffer. The cells were washed and blocked for 15 min on ice and then incubated with FITC conjugated goat anti- rabbit antibody (ICN) for 30 min on ice. The cells were fixed with 2% paraformaldehyde for 10 minutes at room temperature and then stained with 1 μg/ml DAPI in PBS for 5 minutes at room temperature. The coverslips were mounted in 50% glycerol in PBS containing 0.1% anti-fading reagent and observed under a confocal microscope. Results show DAPI (blue) or anti-fibronectin antibody (green) staining under visible (top) or fluorescent (bottom) illumination. **B.** FACS analysis of fibronectin expression on fibroblast APCs and adhesion molecules on purified T cells. The fibroblasts were negative for fibronectin expression (dotted line) whereas T cells

expressed high levels of CD62L (bold line) and CD102 (ICAM-2, bold dotted line) and moderate levels of CD49d (VLA-4, dashed line) and CD49 (VLA-5, dotted line). **C.** T cells loaded with 5 μM Fura-2/AM were mixed with 20 μg/ml CS-1 peptide (EILDVPST) plus 20 μg/ml GRGDS peptide (Bachem, USA) or 10 μg/ml anti-VLA-4 plus 10 μg/ml anti-VLA-5 blocking antibodies (BioLegend). Mean fluorescence ratios (340/380 nm) of T cells bound to CD3L-CD43 APCs in the presence of blocking peptides (RGD and CS-1, dashed line), blocking antibodies (anti-VLA-4 and anti-VLA-5, dotted line) or vehicle (none) with (T or without (NT) micropipette-induce tension on the T cells are shown. Addition of peptides or antibodies that block VLA-4/VLA-5 interactions with fibronectin did not reduce the calcium response induced by tensive forces acting on T cells immobilized via the TCR complex, indicating that signaling through VLA-4 and VLA-5 was not responsible for the observed calcium mobilization in T cells.

Figure S3. Mechanical forces acting on B3Z T cells bound via immobilized CD3L-CD43 protein can induce calcium responses. A, Purified CD3L-CD43 protein (0.5 for HA staining or 5 μg for anti-His staining) was electrophoresed on a SDS-PAGE (upper panel) or transferred to a nitrocellulose membrane and immunoblotted with anti-HA or anti-His antibody (lower panel). **B,** Glass coverslips cleaned with HNO_3 and KOH were

immersed in 0.01% acetic acid containing 2% (vol/vol) 3-glycidyloxypropyl-trimethoxysilane (Aldrich Chemical Company) for 3 h at 95°C. After washing with water, the coverslips were incubated in 0.01 M $NaHCO_3$ (pH 10.0) containing 10% (wt/vol) *N*-(5-amino-1-carboxypentyl)-iminodiacetic acid (Sigma) for 16 h at 60°C. The slides were washed with water and then incubated in 10 mM $NiCl_2$ and 5 mM glycine (pH 8.0) for 2 h at room temperature and then washed with water. NTA-derivatized coverslips were treated with binding buffer (5 mM imidazole, 0.5 M NaCl, 20 mM Tris-HCl pH 7.9) for 30 minutes at room temperature and washed with washing buffer (30 mM imidazole, 0.5 M NaCl, 20 mM Tris-HCl pH 7.9). Glass cover slips were incubated with 100 μg/ml CD3L-CD43-his protein for 1 h at room temperature and then extensively washed. Binding of CD3L-CD43-his on coverslips was assessed by sequential incubation with rat anti-HA (3F10, Roche) and Qdot® 655 anti-rat IgG secondary antibody (Invitrogen) for 45 min at room temperature. Imaging was performed using a 100X oil immersion objective (Olympus) and a CCD camera controlled by Velocity (Perkin Elmer, USA). The average density was 1.1 Qdots per μm^2. **C,** Mean fluorescence ratio (340/380 nm) of fura-2/AM B3Z T cells bound to CD3L-CD43 proteins on glass slides with (T) or without (NT) micropipette-induced tension on the cells. The results show B3Z cells that display calcium responses after tensive forces were initiated (12 of 20 B3Z T cells).

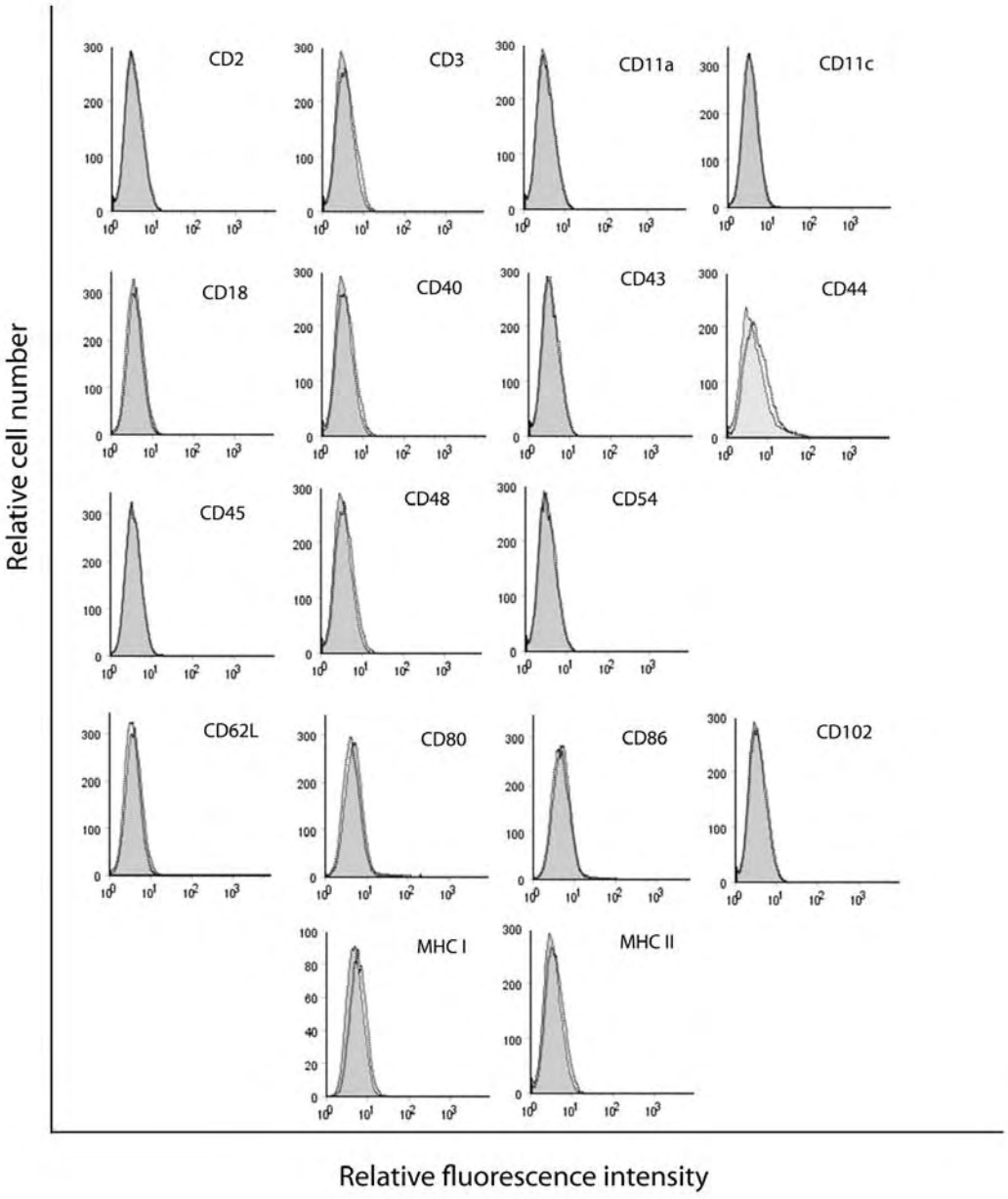
CD2
CD3
CD11a
CD11c
CD18
CD40
CD43
CD44
CD45
CD48
CD54
CD62L
CD80
CD86
CD102
MHC I
MHC II
Relative cell number
Relative fluorescence intensity

Figure S1

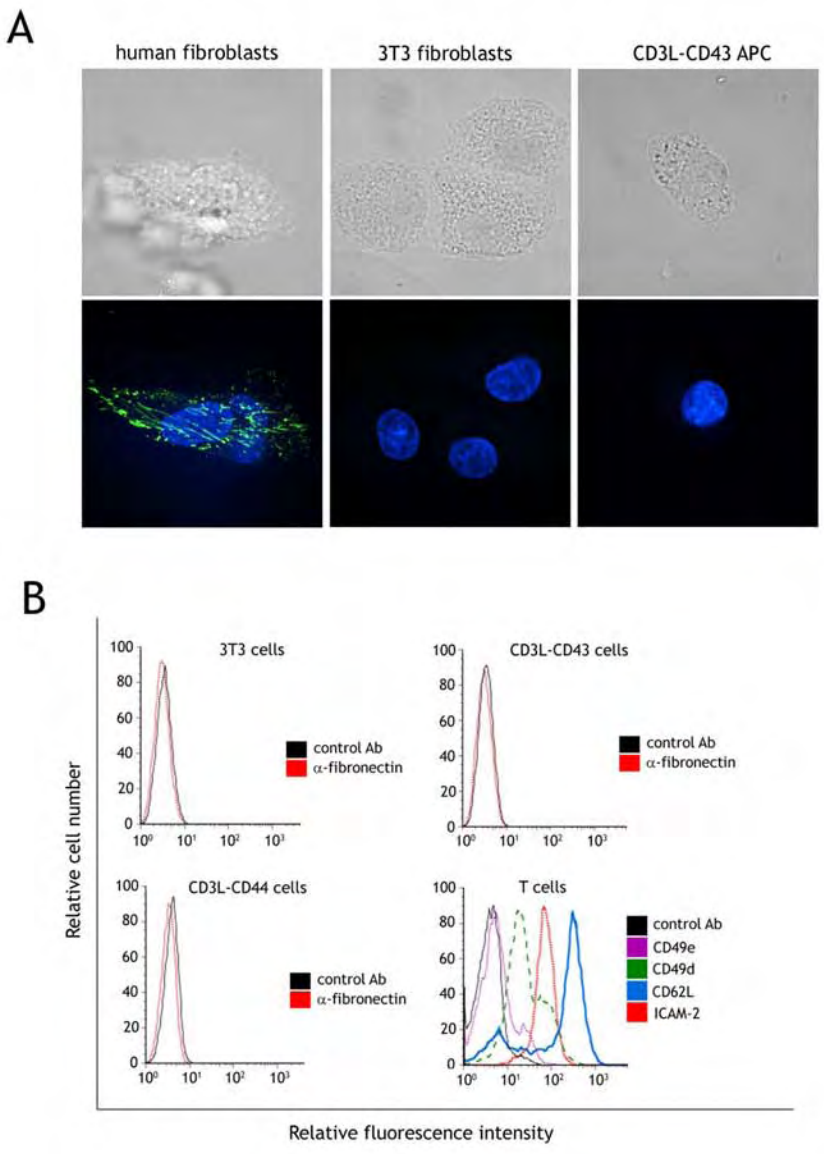

Supplemental Figure 2

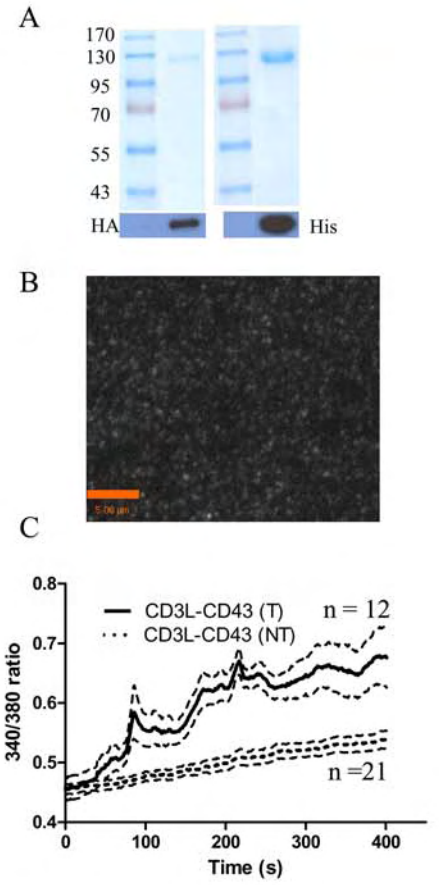

Li et al., Supplemental Figure 3